The influence of loading path on fault reactivation: a laboratory perspective

C. Giorgetti[1], and M. Violay[1]

[1]Laboratory of Experimental Rock Mechanics, ENAC, EPFL Lausanne, Switzerland

Abstract: Although natural faults are variably oriented to the Earth's surface and to the local stress field, the mechanics of fault reactivation and slip under variable loading paths (sensu Sibson, 1993) is still poorly understood. Nonetheless, different loading paths commonly occur in natural faults, from load-strengthening when the increase in shear stress is coupled with an increase in normal stress (e.g., reverse faults in the absence of fluid pressure increase) to load-weakening when the increase in shear stress is coupled with a decrease in normal stress (e.g., normal faults). According to the Mohr-Coulomb theory, the reactivation of pre-existing faults is only influenced by the fault orientation to the stress field, the fault friction, and the principal stresses magnitude. Therefore, the stress path the fault underwent is often neglected when evaluating the potential for reactivation. Yet, in natural faults characterized by thick, incohesive fault zone and highly fractured damage zone, the loading path could not be ruled out. Here we propose a laboratory approach aimed at reproducing the typical tectonic loading paths for reverse and normal faults. We performed triaxial saw-cut experiments, simulating the reactivation of well-oriented (i.e., 30° to the maximum principal stress) and misoriented (i.e., 50° to the maximum principal stress), normal and reverse gouge-bearing faults under dry and water-saturated conditions. We find that load-strengthening versus load-weakening path results in clearly different hydro-mechanical behaviour. Particularly, prior to reactivation, reverse faults undergo *compaction* even at differential stresses well below the value required for reactivation. Contrarily, normal faults experience *dilation*, most of which occurs only near the differential stress values required for reactivation. Moreover, when reactivating at comparable normal stress, normal faults (load-weakening path) are more prone to slip seismically than reverse fault (load-strengthening path). Indeed, the higher mean stress that normal fault experienced before reactivation compacts more efficiently the gouge layer, thus increasing the fault stiffness and favouring seismic slip. This contrasting fault zone compaction and dilation prior to reactivation may occur in different natural tectonic settings, affecting the fault hydro-mechanical behaviour. Thus, taking into account the loading path the fault underwent is fundamental in evaluating both natural and induced fault reactivation and the related seismic risk assessment.

EGU General Assembly 2020

Theoretical background and motivation

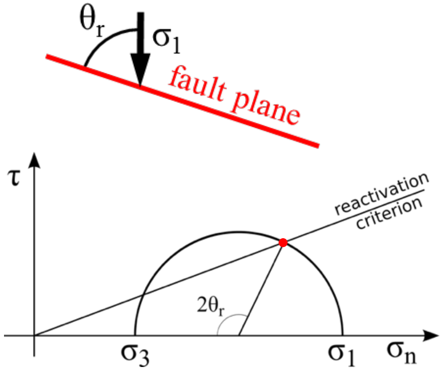

Faults in the brittle crust constitute pre-existing weakness planes.

Fault reactivation occurs whenever the resolved shear stress on the fault plane overcomes the fault frictional strength (e.g., Jaeger, 1960; Sibson, 1985).

This condition only depends on the fault friction (μ), the angle between the fault plane and the maximum principal stress axis (θ), and the magnitude of the principal stresses (σ_1, σ_2, σ_3).

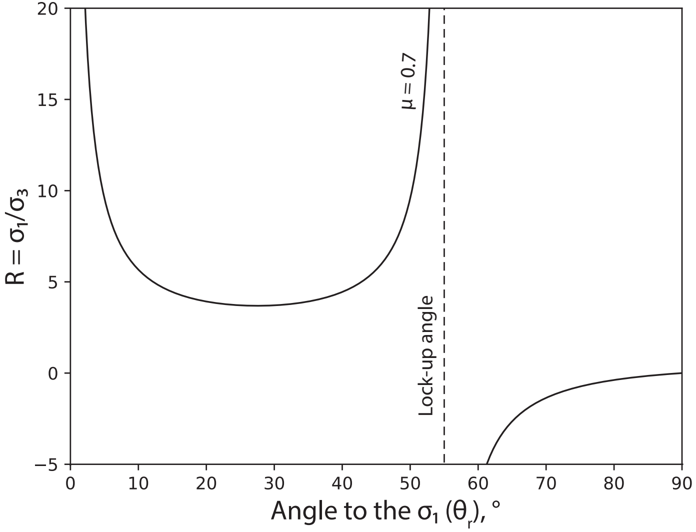

The stress ratio required for reactivation is evaluated as follow:

$$R = \frac{\sigma_1}{\sigma_3} = \frac{1 + \mu_s \cot\theta}{1 - \mu_s \tan\theta}$$

This approach assumes that faults are *zero-thickness* planes.

Although this simple approach is reliable, it does not take into account the loading path the fault experienced before reactivation.

Recent studies (e.g., Schorlemmer et al., 2015; Petruccelli et al., 2019) show that the faulting type (normal, strike-slip, or reverse), and thus the loading path, influences the seismic behaviour of faults.

In natural faults characterized by thick, incohesive fault zone and highly fractured damage zone, the loading path could not be ruled out.

Venere fault (central Italy)
e.g., Agosta and Aydin, 2006

Methods

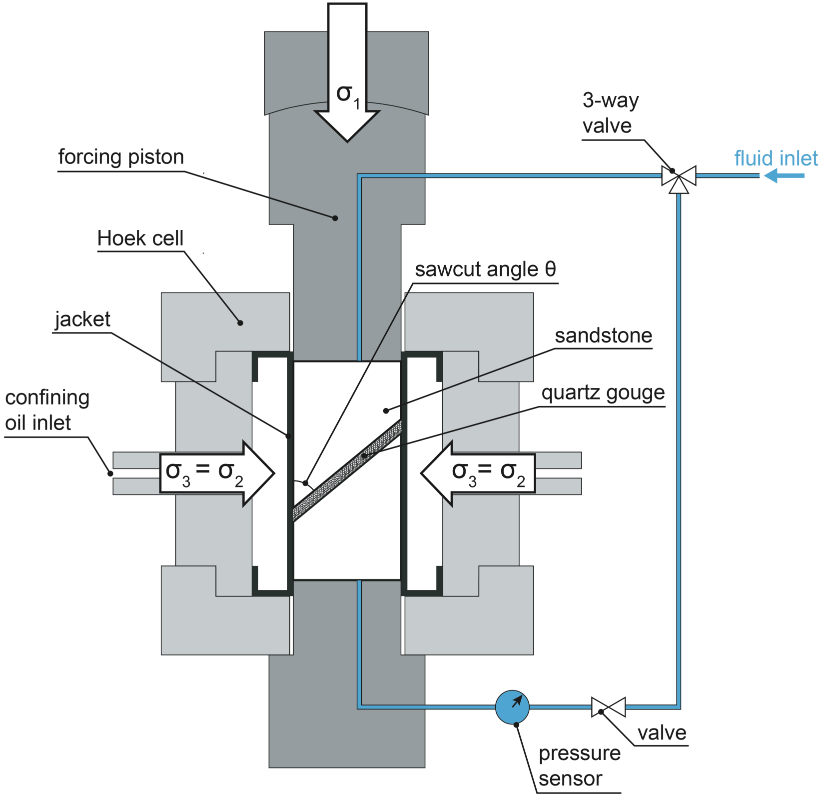

To investigate the role of the loading path on gouge-bearing fault reactivation, we performed triaxial saw-cut experiments.

Experimental conditions:

- saw-cut angle: **30°** (well-oriented) and **50°** (misoriented) to the σ_1;
- **dry** (room humidity) and **water** saturated;
- room temperature.

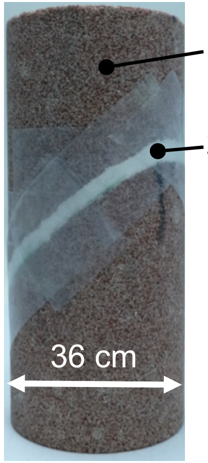

Methods

First, the sample is isotropically loaded at a rate of 0.033 MPa/s to the target σ_3 and P_f for load-strengthening experiments and the target σ_1 and P_f for load-weakening experiments.

Once the initial isotropic pressure is achieved, load-strengthening and load-weakening paths were imposed to the sample, respectively increasing the maximum principal stress or decreasing the minimum principal stress at a constant loading/unloading rate $\delta\sigma_1/\delta t$ or $\delta\sigma_3/\delta t$.

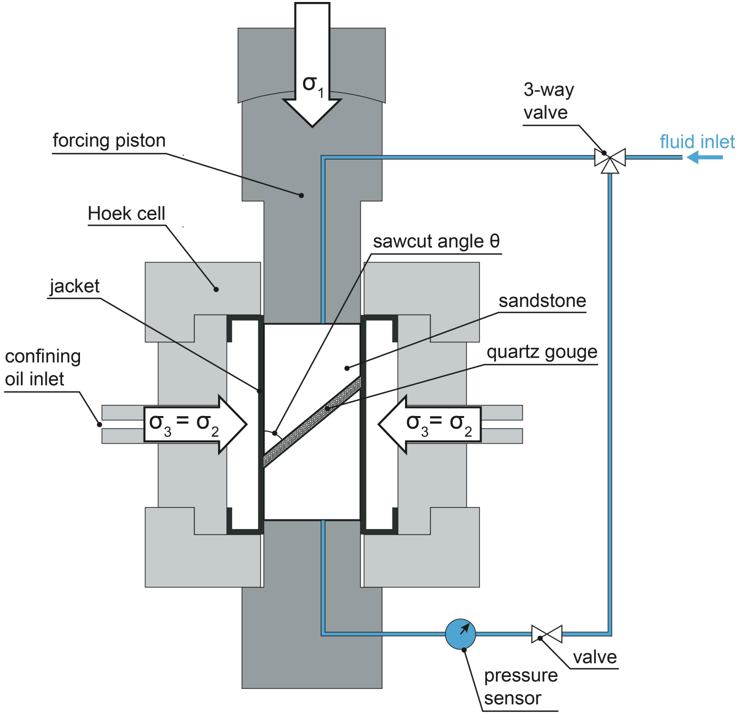

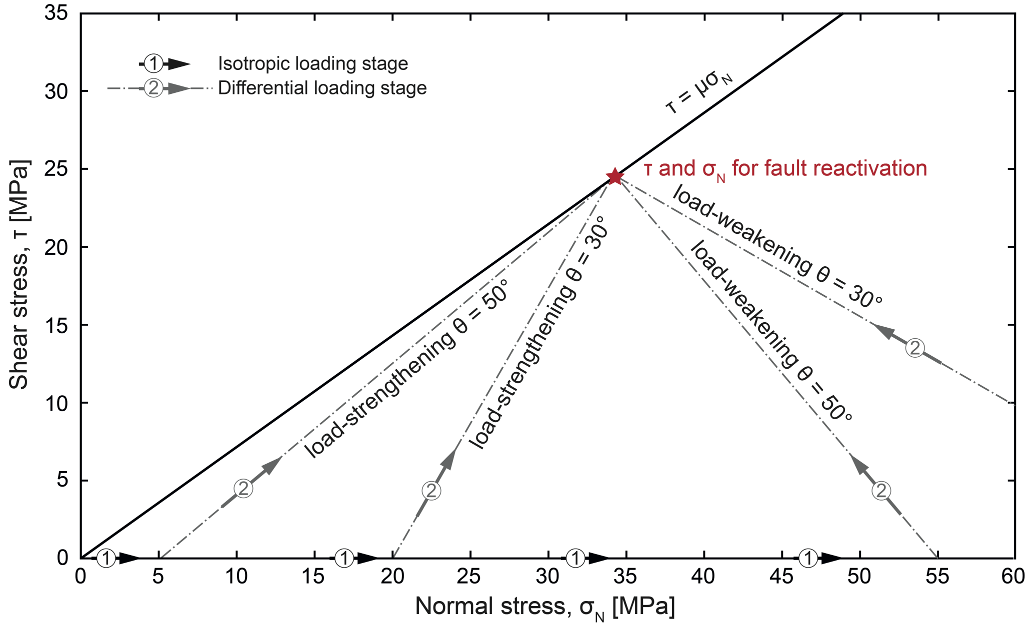

Methods

The imposed loading/unloading rates $\delta\sigma_1/\delta t$ and $\delta\sigma_3/\delta t$ range between 0.0035 MPa/s and 0.0100 MPa/s to achieve reactivation after a comparable amount of time following different loading paths. The starting isotropic pressure values were chosen in order to achieve reactivation at the same normal stress for faults undergoing load-strengthening (LS) and load-weakening (LW) path. The tested normal stresses at reactivation are $\sigma_n \approx$ 12-35 MPa.
In water-saturated experiments the pore pressure is maintained constant during the experiments in order to result in a pore fluid factor λ=0.3, equal to Pf/σ_3 in load-strengthening path and to Pf/σ_1 in load-weakening path (e.g., Sibson, 1993).

θ	hydrostatic P_c (MPa)	Pf (MPa)	loading path	rate	σ_n at reactivation
50°	5	0	LS	0.010 MPa/s	≈ 35 MPa
50°	55	0	LW	0.010 MPa/s	≈ 35 MPa
30°	20	0	LS	0.009 MPa/s	≈ 35 MPa
50°	30	0	LW	0.006 MPa/s	≈ 20 MPa
30°	10	0	LS	0.007 MPa/s	≈ 20 MPa
30°	45	0	LW	0.007 MPa/s	≈ 20 MPa
30°	42.9	12.9	LW	0.0046 MPa/s	≈ 12 MPa
30°	10	3	LS	0.0046 MPa/s	≈ 12 MPa
50°	28	8.4	LS	0.0034 MPa/s	≈ 12 MPa
50°	48.6	14.6	LW	0.0062 MPa/s	≈ 22 MPa
50°	4.3	1.3	LS	0.0062 MPa/s	≈ 22 MPa

Results: dry experiments

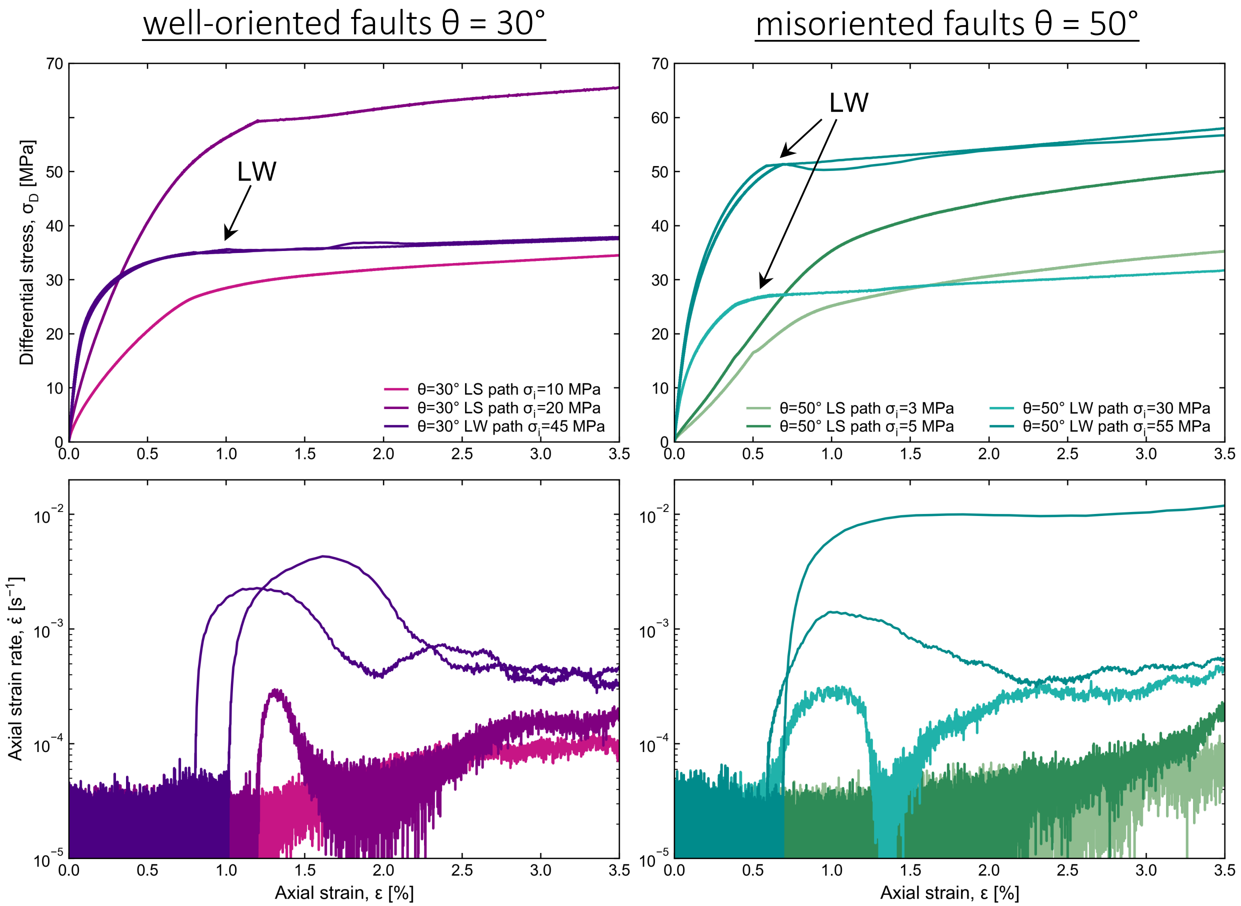

- Under load-weakening (LW) path faults appear stiffer than under load-strengthening (LS) path.
- Under LW path, once the differential stress for reactivation is achieved, the fault suddenly accelerates.
- Under LS path, once the differential stress for reactivation is achieved, the fault creeps continuously and smoothly accelerates.

Giorgetti and Violay, to be submitted

Results: water saturated experiments

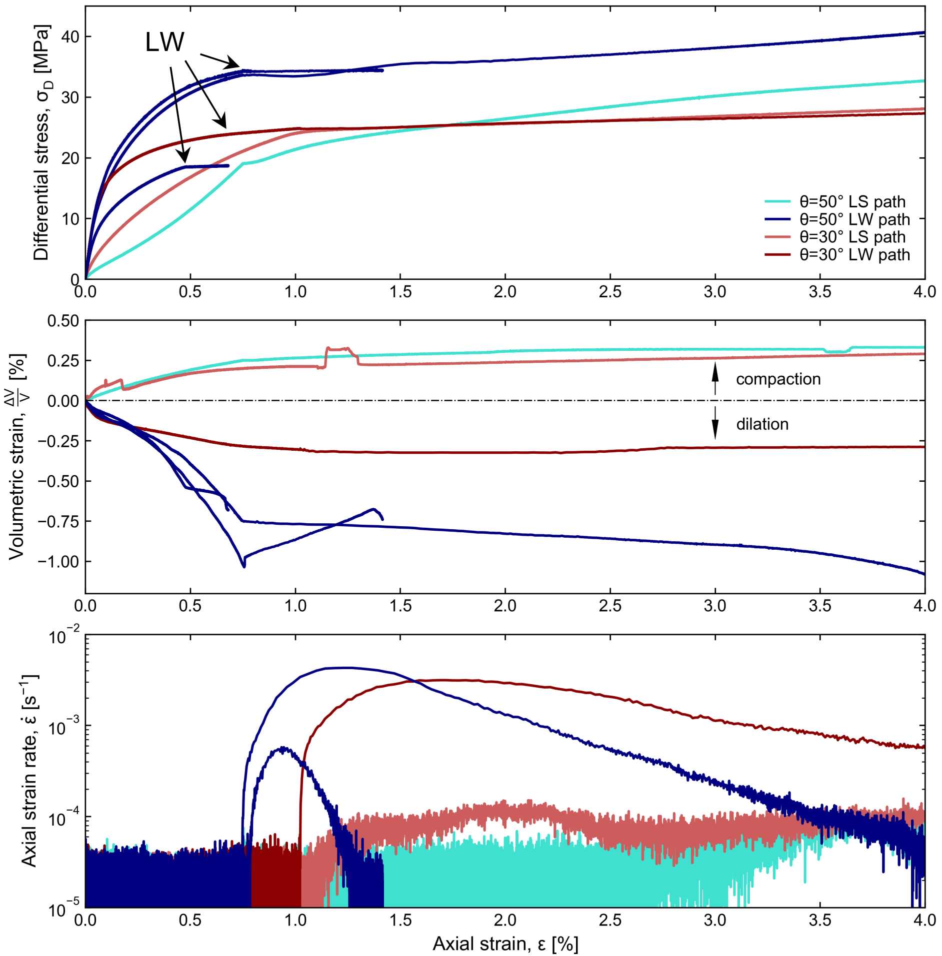

- The results are consistent with the observations collected from dry experiments.
- The fault gouges experiencing load-strengthening path undergo *compaction* until the steady-state differential stress is attained.
- Load-weakening paths result in *dilation* of the fault gouge during the differential stress increase before the abrupt fault acceleration.

Giorgetti and Violay, to be submitted

Results: summary on Mohr-Coulomb plane

Under LS path, the deformation starts to slowly accelerate at lower shear stress, especially for misoriented faults, with the only exception of the experiment conducted at 20 MPa of confining pressure (σ_3) under dry conditions.
Under LW path, the deformation abruptly accelerates only when the stresses for reactivation are reached, with the only exception of the experiment conducted at ~19 MPa of axial stress (σ_1) under wet conditions.

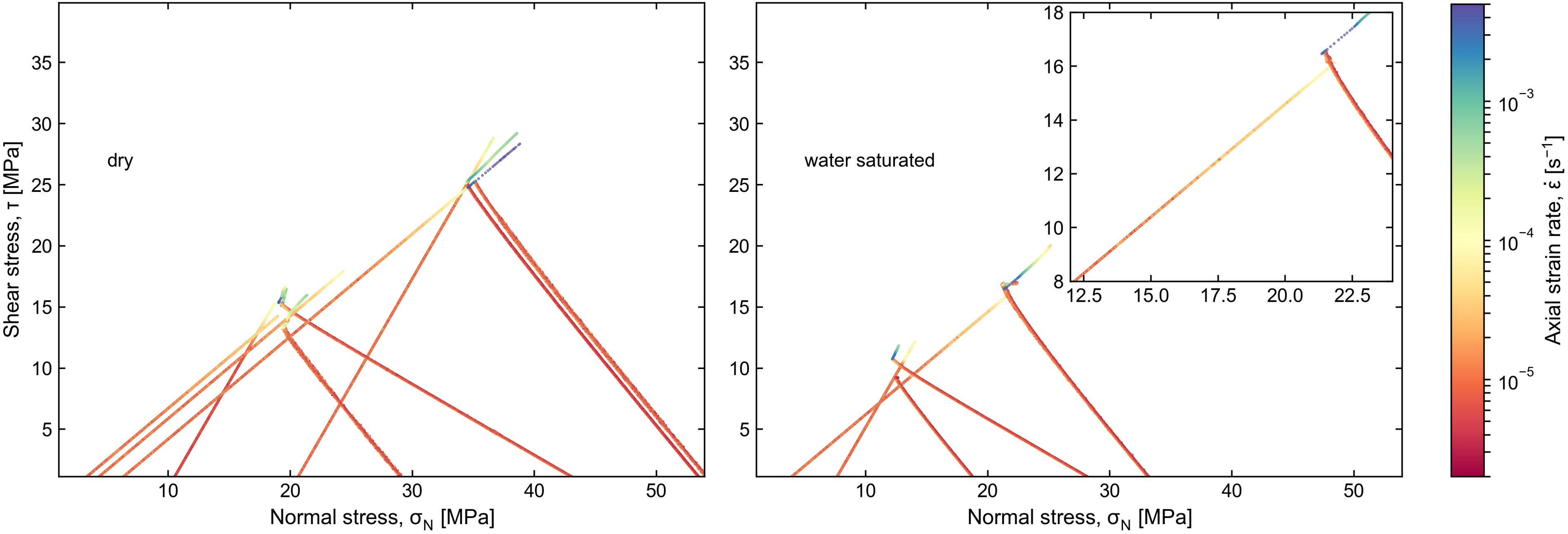

Giorgetti and Violay, to be submitted

Discussion

The observed behaviour suggests that faults undergoing LW path (normal faults) tend to slip seismically, whereas faults undergoing LS path (reverse faults) tend to slip aseismically. To understand this behaviour, we investigated the interplay between the elastic properties of the fault gouge and the elastic properties of the surrounding sandstone.

We experimentally measured the shear modulus of the intact sandstone at different confining pressure under dry conditions, through the measurement of ultrasonic wave velocities.
We inferred the evolution of the shear modulus of the fault gouge, from the change in porosity estimated during the isotropic pressure increase under dry conditions.

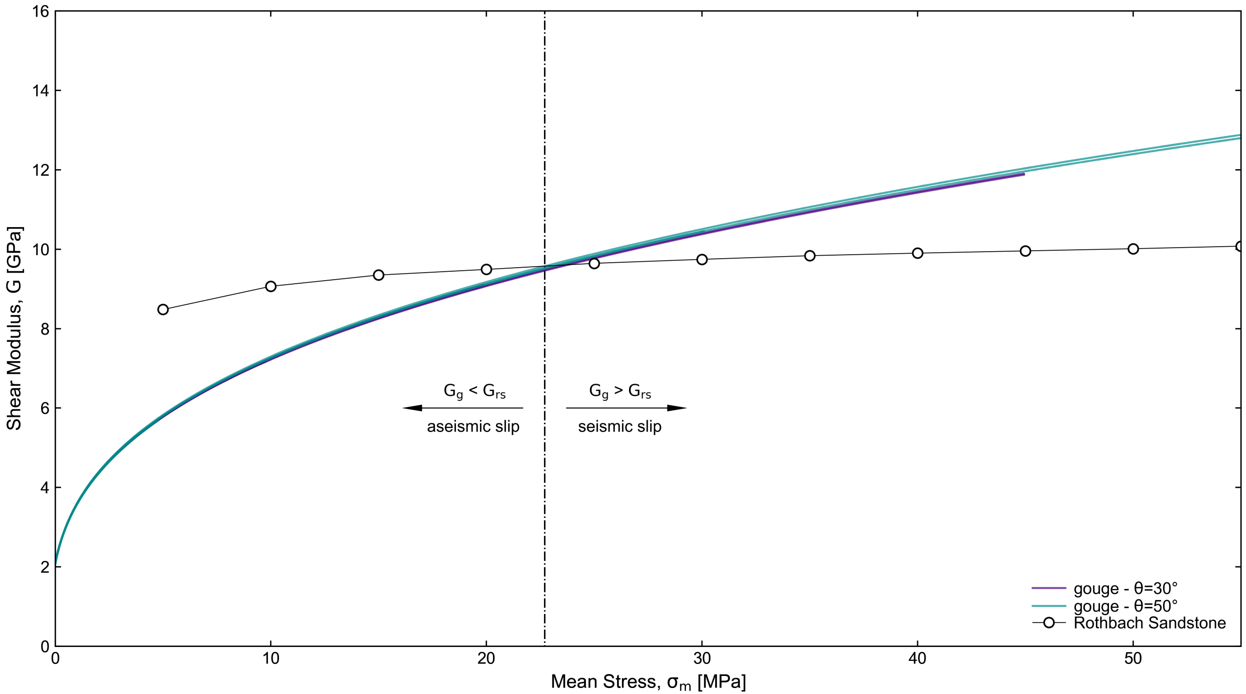

Giorgetti and Violay, to be submitted

The change in porosity is calculated from the axial deformation measured during the experiments, assuming that all deformation measured originates from porosity loss in the gouge.

The shear modulus is evaluated as follow (Walton, 1987):

$$G_{gouge} = \frac{3}{5}\sqrt[3]{\frac{C^2(1-\varphi)^2 G^2}{18\pi^2(1-\nu)^2}\sigma_m}$$

C = 6. coordination number
G = 44.0 GPa shear modulus of quartz mineral grains
ν = 0.07 Poisson's ratio of quartz mineral grains
σ_m = mean stress

There is a critical value of mean stress σ_m for higher values of which the fault gouge becomes stiffer than the surrounding sandstone. Consistently, the limit separates seismic to aseismic behaviour.

Conclusions

- Under load-strengthening conditions, faults start to creep at differential stress values that are lower than the values required for the abrupt acceleration of the fault under load weakening conditions.
- Before reactivation, reverse faults undergo *compaction*, whereas normal faults experience *dilation.*
- When reactivating at comparable normal stress, normal faults (load-weakening path) are more prone to slip seismically than reverse fault (load-strengthening path).
- The higher mean stress that normal faults (load-weakening path) experienced before reactivation compacts more efficiently the gouge layer, thus increasing fault stiffness and favouring seismic slip.
- The stress path history of a fault may influence its seismic behaviour, especially if in the presence of a thick gouge-bearing fault zone.

- Thank you for reading! -

Thanks to:

Schweizerische Eidgenossenschaft
Confédération suisse
Confederazione Svizzera
Confederaziun svizra

Bundesamt für Energie BFE
Office fédéral de l'énergie OFEN

References

Agosta, F., & Aydin, A. (2006). Architecture and deformation mechanism of a basin-bounding normal fault in Mesozoic platform carbonates, central Italy. *Journal of Structural Geology*, **28**(8), 1445-1467. https://doi.org/10.1016/j.jsg.2006.04.006

Bésuelle, P., Baud, P., & Wong, T. F. (2003). Failure mode and spatial distribution of damage in Rothbach sandstone in the brittle-ductile transition. In *Thermo-Hydro-Mechanical Coupling in Fractured Rock* (pp. 851-868). Birkhäuser, Basel. https://doi.org/10.1007/978-3-0348-8083-1_4

Jaeger, J. C. (1960). Shear failure of anisotropic rocks. *Geological Magazine*, **97**, 65-72. https://doi.org/doi:10.1017/S0016756800061100

Petruccelli, A., Gasperini, P., Tormann, T., Schorlemmer, D., Rinaldi, A. P., Vannucci, G., & Wiemer, S. (2019). Simultaneous dependence of the earthquake-size distribution on faulting style and depth. *Geophysical Research Letters*, **46**, 11044-11053. https://doi.org/10.1029/2019GL083997

Schorlemmer, D., Wiemer, S. & Wyss, M. (2005). Variations in earthquake-size distribution across different stress regimes. *Nature,* **437,** 539-542. https://doi.org/10.1038/nature04094

Sibson, R. H. (1985). A note on fault reactivation. *Journal of Structural Geology*, **7**(6), 751-754, https://doi.org/doi:10.1016/0191-8141(85)90150-6

Sibson, R. H. (1993). Load-strengthening versus load-weakening faulting. *Journal of Structural Geology*, **15**(2), 123-128. https://doi.org/10.1016/0191-8141(93)90090-W

Walton K. (1987). The effective elastic moduli of a random packing of spheres. *Journal of the Mechanics and Physics of Solids*, **35**, 213-226. https://doi.org/10.1016/0022-5096(87)90036-6